

Rethinking Irregular Time Series Forecasting: A Simple yet Effective Baseline

Xuyuan Liu*, Xiangfei Qiu*, Xingjian Wu, Zhengyu Li, Chenjuan Guo, Jilin Hu†, Bin Yang

Abstract

The forecasting of irregular multivariate time series (IMTS) is a critical task in domains like healthcare and climate science. However, this task faces two significant hurdles: 1) the inherent non-uniformity and missing data in IMTS complicate the modeling of temporal dynamics, and 2) existing methods often rely on computationally expensive architectures. To address these dual challenges, we introduce APN, a general and efficient forecasting framework. At the core of APN is a novel Time-Aware Patch Aggregation (TAPA) module that introduces an aggregation-based paradigm for adaptive patching, moving beyond the limitations of fixed-span segmentation and interpolation-based methods. TAPA first learns dynamic temporal boundaries to define data-driven segments. Crucially, instead of resampling or interpolating, it directly computes patch representations via a time-aware weighted aggregation of all raw observations, where weights are determined by each observation's temporal relevance to the segment. This approach provides two key advantages: it preserves data fidelity by avoiding the introduction of artificial data points and ensures complete information coverage by design. The resulting regularized and information-rich patch representations enable the use of a lightweight query module for historical context aggregation and a simple MLP for final prediction. Extensive experiments on multiple real-world datasets demonstrate that APN establishes a new state-of-the-art, significantly outperforming existing methods in both prediction accuracy and computational efficiency.

1 Introduction

Irregular Multivariate Time Series (IMTS) data are widely observed in various domains such as healthcare, biomechanics, climate science, and astronomy (Yao, Bi, and Chen 2018; Brouwer et al. 2019; Kidger et al. 2020; Ham, Kim, and Luo 2019; Vio, Díaz-Trigo, and Andreani 2013). Irregular Multivariate Time Series Forecasting (IMTSF) is a crucial research task that provides valuable insights for early warning and proactive decision-making. However, the inherent irregularity of observations and missing data (Yalavarthi et al. 2024; Zhang et al. 2024) in IMTS pose significant challenges to IMTSF modeling.

To address this challenge, recent IMTSF methods, such as T-PatchGNN (Zhang et al. 2024) and TimeCHEAT (Liu, Cao, and Chen 2025), have adopted the Fixed Patching approach—see Figure 1a. This approach divides the time

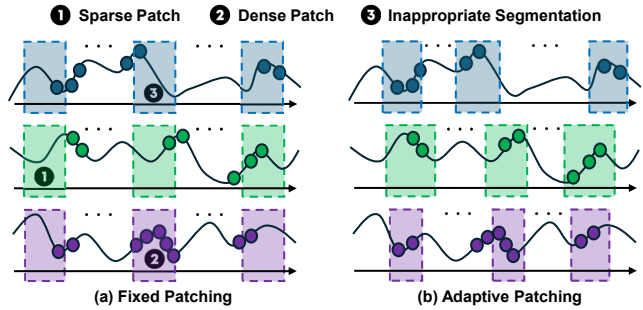


Figure 1: Fixed Patching vs. Adaptive Patching.

series into fixed-length patches with equal intervals among them. However, this approach has notable limitations: 1) *Uneven Information Density Across Patches*: Fixed Patching struggles to adapt to local variations in data density, leading to uneven information density among patches. For example, sparse patches (where the number of observations is limited) may result in insufficient feature extraction, yet dense patches (where the number of observations is abundant) may contain redundant information or noise, thereby impairing the extracted features. 2) *Inappropriate Segmentation of Key Semantic Information*: Fixed Patching risks splitting critical dynamic information, which hampers the model's ability to capture the complete semantic context. Therefore, **the first challenge is to design an adaptive patching approach that can effectively adapt to local information density variations in IMTS and capture the complete semantic context.**

Meanwhile, existing IMTSF models generally suffer from high computational costs and long running times. For example, neural ODEs-based models (Chen et al. 2018; Rubanova, Chen, and Duvenaud 2019; Gravina et al. 2024) require computationally intensive numerical solvers to accurately model continuous-time dynamics (Shukla and Marlin 2021; Chen et al. 2018). GNNs-based models (Yalavarthi et al. 2024; Zhang et al. 2024) are hindered by the overhead of complex graph construction and multi-round node information aggregation (Wu et al. 2021); Transformer-based models (Chen et al. 2023; Zhang et al. 2023), which utilize multi-layer self-attention mechanisms and feedforward networks, often result in large parameter scales (Kim et al.

2024). These models typically construct computationally intensive and parameter-heavy complex architectures to effectively handle the intricate dependencies and dynamic changes in IMTS. While this design enhances the model’s performance to some extent, it also incurs high computational costs and long runtimes, limiting its practical application in resource-constrained scenarios. Notably, in regular time series forecasting task, models such as DLinear (Zeng et al. 2023), SparseTSF (Lin et al. 2024b), and CycleNet (Lin et al. 2024a) have significantly reduced computational overhead and achieved competitive prediction accuracy by adopting simple architectures with fewer parameters. Therefore, **the second challenge is to design a model for IMTSF that is both highly accurate and computationally efficient.**

To address the above challenges, we propose a general framework called APN. Specifically, we design a novel Time-Aware Patch Aggregation (TAPA) module that achieves adaptive patching—see Figure 1b. Unlike methods that resample data points within a patch, TAPA directly aggregates the raw, irregular observations. It learns dynamically adjustable patch boundaries to flexibly frame regions of interest. Crucially, it then employs a time-aware soft-weighting mechanism to generate a patch representation, ensuring that all observations are holistically considered and contribute to the representation based on their temporal relevance to the patch. This approach not only adapts to local information density and captures complete semantic units but also inherently prevents information loss by design, as no data point is left uncovered. Based on these high-quality representations, we use a simple query module to effectively integrate historical information while maintaining the model’s efficiency. Finally, predictions are made by a shallow MLP. Results on multiple real-world datasets show that APN outperforms existing state-of-the-art methods in both efficiency and accuracy.

The contributions of our paper are summarized as follows:

- To address the IMTSF, we propose a general framework named APN. This framework leverages adaptive patching to generate high-quality and regular initial patch representations. Based on these representations, we employ a simple query module to integrate contextual information, enabling a lightweight yet powerful overall architecture.
- We design a novel TAPA module to achieve adaptive patching. By learning dynamic patch boundaries and employing a time-aware soft-aggregation scheme over raw observations, TAPA produces high-quality regularized representations without interpolation. This mechanism effectively adapts to local variations in information density, captures complete semantics, and guarantees full coverage of all data points.
- We conduct extensive experiments on multiple datasets. The results show that APN outperforms existing SOTA baselines in both forecasting accuracy and computational efficiency.

2 Related Work

2.1 Irregular Multivariate Time Series Forecasting

IMTSF is crucial for key domains such as healthcare and climate science. The inherent characteristics of IMTS, such as non-uniform sampling intervals and asynchronous channels, present significant challenges to regular time series forecasting models. To address these characteristics, researchers have proposed various IMTSF models. Some models employ approaches based on continuous-time dynamics (Chen et al. 2018; Rubanova, Chen, and Duvenaud 2019; Schirmer et al. 2022; Brouwer et al. 2019), utilizing ordinary or stochastic differential equations (ODE/SDE) to adapt to irregular sampling points. For instance, Neural Flows (Bilios et al. 2021) proposes directly modeling the solution curves of ODEs, thereby avoiding the costly numerical integration steps in traditional ODE solvers. GRU-ODE-Bayes (Brouwer et al. 2019) innovatively combines the idea of Gated Recurrent Units (GRU) with ODEs and effectively handles sparse observational data through a Bayesian update mechanism. Other models leverage graph neural networks and attention mechanisms (Yalavarthi et al. 2024; Zhang et al. 2024; Liu, Cao, and Chen 2025) to capture complex dependencies in IMTS. For example, GraFITi (Yalavarthi et al. 2024) transforms IMTS into sparse bipartite graphs and predicts edge weights through GNNs. T-PatchGNN (Zhang et al. 2024) innovatively segments irregular sequences into time-aligned patches and combines Transformer and adaptive GNNs to handle intra-patch and inter-patch dependencies, respectively.

2.2 Progress in Patch-based Irregular Multivariate Time Series Forecasting

The patch-based strategy, which has proven successful for regular time series (Nie et al. 2023; Wang et al. 2022), has been adapted for IMTS Forecasting (IMTSF). Initial adaptations, such as T-PatchGNN (Zhang et al. 2024) and TimeCHEAT (Liu, Cao, and Chen 2025), employed a fixed-span patching strategy. However, this rigid segmentation is ill-suited for the non-uniform data distribution of IMTS. It often creates patches with highly variable information content—some being too sparse for meaningful feature extraction, while others may be overly dense with redundant data.

To overcome this, adaptive patching emerged as a natural evolution. One prominent approach, primarily explored in the context of regular time series (e.g., HDMixer (Huang et al. 2024)), involves learning flexible patch boundaries and then generating regularized patch representations through interpolation-based resampling. While effective for dense, regular data, this methodology is fundamentally flawed for IMTS. Interpolating across sparse or missing intervals can fabricate misleading data points, introducing significant artifacts and undermining model reliability.

In contrast, our work proposes a distinct aggregation-based adaptive patching paradigm, specifically designed for the challenges of IMTS. Instead of creating new, artificial data points, our TAPA module learns dynamic “soft

windows" and computes each patch representation by performing a direct, weighted aggregation of all original observations. This strategy provides two critical advantages for IMTS:(1)Data Fidelity: It exclusively uses the original, observed data, thereby avoiding the distortions and potential inaccuracies of interpolation.(2)Complete Information Coverage: The soft-weighting mechanism ensures that every data point contributes to the representation of relevant patches, mathematically precluding the information loss that can occur when observations fall between the hard boundaries of other methods.

3 Methodology

3.1 Problem Definition

An Irregular Multivariate Time Series (IMTS) \mathcal{O} consists of N independent univariate sequences $\{o_{1:L_n}^n\}_{n=1}^N$. Each sequence $o_{1:L_n}^n$ comprises L_n observations (t_i^n, v_i^n) , where the intervals between timestamps t_i^n are irregular, and sampling across different variables is typically asynchronous. The IMTS forecasting task is defined as: given historical observations \mathcal{O} and a set of prediction queries for all variables $\mathcal{Q} = \{[q_j^n]_{j=1}^{Q_n}\}_{n=1}^N$, construct and optimize a prediction model $\mathcal{F}(\cdot)$ capable of accurately predicting the future observed values $\hat{\mathcal{V}} = \{[\hat{V}_j^n]_{j=1}^{Q_n}\}_{n=1}^N$ corresponding to each query q_j^n , i.e.:

$$\mathcal{F}(\mathcal{O}, \mathcal{Q}) \rightarrow \hat{\mathcal{V}} \quad (1)$$

3.2 Framework Overview

The architectural design of APN is guided by a core principle: decoupling the challenge of handling irregularity from the task of forecasting. As illustrated in Figure 2, instead of relying on a monolithic, complex model, APN adopts a strategic two-stage pipeline.

The cornerstone of this pipeline is the *Time-Aware Patch Aggregation* (TAPA) module (Section 3.3). Operating in a channel-independent manner, its sole yet critical purpose is to transform the raw, irregular observations into a high-quality, regularized sequence of patch representations. Through its novel use of *Adaptive Patching* and *Weighted Aggregation*, TAPA robustly adapts to local information density and captures complete semantic units. Crucially, it achieves this without resorting to interpolation, thereby preserving data fidelity and sidestepping the introduction of artificial artifacts.

The success of this initial transformation is pivotal, as it enables the subsequent use of a remarkably efficient and lightweight architecture. A concise *Query-based Aggregation* module (Section 3.4) then effectively summarizes the historical context from these regularized patches for each variable. Finally, this compact representation is fed into a simple MLP-based *Forecasting Decoder* (Section 3.5) for the final prediction.

In essence, APN strategically front-loads the complexity of handling irregularity into the novel TAPA module. By producing information-rich, regularized representations upfront, it obviates the need for computationally expensive

back-end models, achieving state-of-the-art performance through an elegant and efficient design.

3.3 Time-Aware Patch Aggregation (TAPA)

At the heart of APN lies the Time-Aware Patch Aggregation (TAPA) module, a novel mechanism designed to fundamentally reframe how we process irregular time series. Traditional methods rely on a paradigm of "hard segmentation," imposing rigid, fixed-span boundaries that are ill-suited to the non-uniform nature of IMTS. In stark contrast, TAPA introduces a "soft aggregation" paradigm. Instead of discretely assigning observations to patches, it conceptualizes each patch as a soft, overlapping field of influence, allowing it to aggregate information from all observations in a temporally-aware manner.

This paradigm shift is realized through a cohesive, two-step process executed independently for each channel $X^n = \{(t_i^n, v_i^n)\}_{i=1}^{L_n}$. First, in Adaptive Patching, the model learns the dynamic temporal characteristics—the center and scale—of each patch's field of influence. Second, in Weighted Aggregation, it computes a representation for each patch by performing a direct, weighted aggregation of all raw observations, where the weights are determined by each observation's temporal relevance to the patch's learned characteristics. This entire process transforms the irregular input sequence into a regularized, information-rich sequence of patch representations $H^n = [h_1^n, \dots, h_P^n]$.

Adaptive Patching: Learning Dynamic Temporal Windows The first step is to define the temporal scope of each patch. Instead of imposing pre-defined, rigid boundaries, TAPA learns a dynamic temporal window, $[t_p^{left,n}, t_p^{right,n}]$, for each target patch p . This dynamism is the core mechanism by which TAPA adapts to the non-uniform distribution of data. For instance, in a sparse but critical region, the model can learn to expand a window's width to ensure sparse yet vital signals are encompassed. Conversely, in a dense region with redundant data, a window can be strategically narrowed to focus on the most salient signals, thus preventing dilution from less informative points.

This adaptive process empowers the model to carve out semantically coherent segments from the raw time series, based on the data's inherent structure. To achieve this, for each patch p and channel n , TAPA learns two key parameters: a positional adjustment δ_p^n and a log-scale width parameter λ_p^n . The window boundaries are then computed as:

$$t_p^{left,n} = c_p - \frac{S_{init}}{2} + \delta_p^n, \quad (2)$$

$$t_p^{right,n} = t_p^{left,n} + \exp(\lambda_p^n), \quad (3)$$

where T_{obs} is the time span of the historical observation window, and $c_p = (p - 0.5) \cdot (T_{obs}/P)$ and $S_{init} = T_{obs}/P$ represent the initial reference center and width, respectively. The use of $\exp(\lambda_p^n)$ is a deliberate design choice, ensuring the learned window width remains strictly positive throughout optimization. This dynamic windowing mechanism allows the model to adaptively frame regions of interest, laying the foundation for a more meaningful and robust aggregation in the subsequent step.

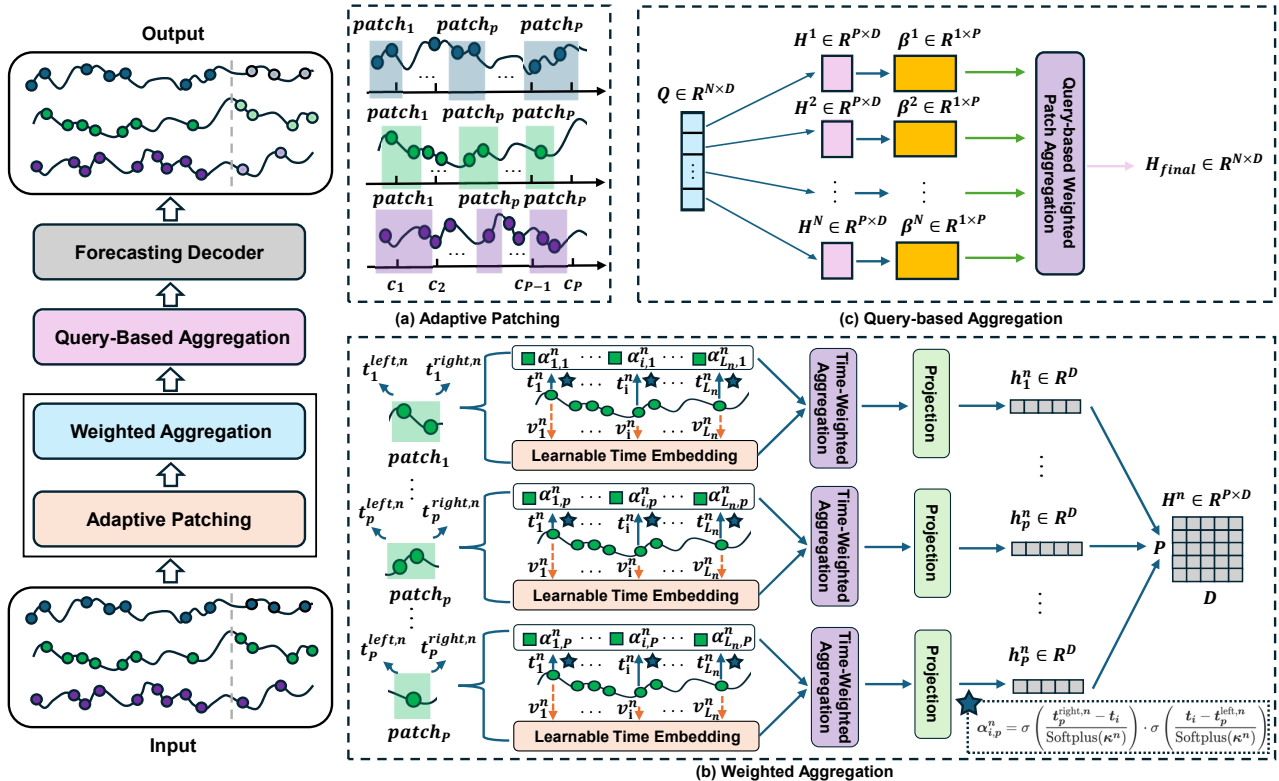


Figure 2: The overall framework of APN, which initially divides each univariate irregular time series into a series of unfixed patches using the *Adaptive Patching* Module. Then the *Weighted Aggregation* Module generates high-quality and regular initial patch representations. Based on the representations, the *Query-based Aggregation* Module is utilized to incorporate contextual information. Finally, the *Forecasting Decoder* outputs the final forecasting results. The *Adaptive Patching* Module and *Weighted Aggregation* Module collectively form the *Time-Aware Patch Aggregation* Module.

Weighted Aggregation: From Raw Observations to Rich Representations With the dynamic temporal windows defined, the next step is to generate patch representations by aggregating information from the raw observations.

Enriching Observations with Temporal Context. To fully leverage temporal information, we first enrich each raw observation. A learnable time embedding, $TE(t_i) \in \mathbb{R}^{D_{te}}$, is generated for each timestamp t_i . This embedding, composed of linear layers for scale and sine-activated layers for periodicity, captures both the absolute position and periodic patterns in time. It is then concatenated with the original value v_i to form an augmented representation: $\tilde{v}_i = \text{Concat}(v_i, TE(t_i))$.

The Soft Window Function. We then employ a time-aware soft window function to calculate the relevance weight, $\alpha_{i,p}^n$, of each observation i to each patch p . The function is elegantly constructed as the product of two Sigmoid functions:

$$\alpha_{i,p}^n = \sigma\left(\frac{t_p^{right,n} - t_i}{\text{Softplus}(\kappa^n)}\right) \cdot \sigma\left(\frac{t_i - t_p^{left,n}}{\text{Softplus}(\kappa^n)}\right). \quad (4)$$

Here, the first Sigmoid term models a smooth "falloff" from the right boundary, while the second models a smooth "rise" from the left boundary. Their product creates a continuous, bell-shaped weighting curve centered within the patch's

learned range. The term $\text{Softplus}(\kappa^n)$ is a learnable, strictly positive temperature that controls the softness of the window edges. A smaller temperature leads to sharper, more defined boundaries, while a larger temperature creates gentler, more overlapping fields of influence, granting the model further adaptive flexibility.

A Crucial Design Choice for Information Integrity. The choice of this soft window function is critical. Since the Sigmoid function $\sigma(x)$ is strictly positive for all real inputs, the resulting weight $\alpha_{i,p}^n$ is also guaranteed to be positive for any observation i and any patch p . This property is not a mere side effect; it is a fundamental design principle that mathematically guarantees complete information coverage. Every observation contributes to the representation of every patch (albeit with varying degrees of influence), inherently preventing the information loss that plagues all hard-segmentation methods where observations can be inadvertently discarded.

Final Aggregation. The final representation for the p -th patch, \bar{h}_p^n , is computed as a normalized weighted average of all augmented observation features:

$$\bar{h}_p^n = \frac{\sum_{i=1}^{L_n} \alpha_{i,p}^n \cdot \tilde{v}_i^n}{\sum_{i=1}^{L_n} \alpha_{i,p}^n + \epsilon} \in \mathbb{R}^{1+D_{te}}, \quad (5)$$

where the summation spans all L_n observations, and ϵ ensures numerical stability. Finally, to enhance expressiveness and align dimensions, we project \bar{h}_p^n into the model’s uniform hidden space via a linear layer: $h_p^n = \text{Linear}_D(\bar{h}_p^n)$. Through this entire process, each univariate irregular sequence is transformed into a refined, structurally regularized sequence $H^n = [h_1^n, \dots, h_P^n] \in \mathbb{R}^{P \times D}$.

3.4 Query-based Weighted Aggregation

The TAPA module delivers a sequence of high-quality, regularized patch representations $H^n = [h_1^n, \dots, h_P^n]$. This successfully concludes the first stage of our pipeline: handling irregularity. The second stage, contextualization and forecasting, can now proceed with remarkable efficiency. To this end, we employ a concise query-based aggregation mechanism to distill the entire historical sequence into a single, potent context vector H_c^n .

First, to preserve the sequential order of the patches, standard positional encodings (PE) are added, yielding position-aware representations $H_{pe}^n = H^n + PE$. Then, instead of resorting to complex inter-patch interactions like multi-head self-attention, we introduce a single learnable query vector $q^n \in \mathbb{R}^D$ for each channel. This query acts as a task-specific lens, dynamically assessing the importance of each patch for the final forecast. The importance scores s_p^n are computed via a simple dot product, normalized into weights β^n via Softmax, and used to compute the final context vector H_c^n as a weighted sum:

$$s_p^n = \frac{q^n \cdot (h_{pe,p}^n)^T}{\sqrt{D}} \quad \text{for } p = 1, \dots, P, \quad (6)$$

$$\beta^n = \text{Softmax}(\{s_p^n\}_{p=1}^P), \quad (7)$$

$$H_c^n = \sum_{p=1}^P \beta_p^n h_{pe,p}^n, \quad (8)$$

The resulting summary representations for all channels, $[H_c^1, \dots, H_c^N]$, form the final representation matrix $H_{final} \in \mathbb{R}^{N \times D}$. A layer normalization is then applied to stabilize the input for the decoder. This lightweight aggregation mechanism is a direct testament to our design philosophy: by front-loading the complexity into TAPA, the subsequent modules can be elegantly simple yet powerful.

3.5 Forecasting Decoder

The final step of the APN framework is the ultimate demonstration of its architectural elegance. Having distilled the entire irregular history into a powerful, fixed-size representation H_{final}^n , the forecasting task becomes remarkably straightforward.

The prediction for a query time τ_k is made by a simple two-layer MLP decoder. This decoder takes the concatenated summary representation H_{final}^n and the learnable temporal encoding of the query time, $TE(\tau_k)$, as input to produce the final value \hat{v}_k^n :

$$\hat{v}_k^n = \text{MLP}(\text{Concat}(H_{final}^n, TE(\tau_k))) \in \mathbb{R} \quad (9)$$

The ability to use such a simple decoder is not a limitation but a feature, underscoring the richness of the representation crafted by TAPA and the query aggregator.

The model is trained end-to-end by minimizing the standard Mean Squared Error (MSE) loss between the predicted values \hat{v}_k^n and the ground truth values v_k^n across all channels and query points:

$$\mathcal{L} = \frac{1}{N \cdot Q} \sum_{n=1}^N \sum_{k=1}^Q (\hat{v}_k^n - v_k^n)^2, \quad (10)$$

where Q is the number of query points for each channel.

4 Experiments

4.1 Setup

Datasets: To comprehensively evaluate the model’s performance, we select four widely-used IMTS datasets, including PhysioNet, MIMIC, Activity, and USHCN. These datasets span multiple domains such as healthcare, biomechanics, and climate science. More details of the benchmark datasets are included in Appendix A.1.

Baselines: To comprehensively evaluate the performance of APN, we compare it with nineteen baseline models. These baseline models can be broadly categorized into the following groups: (1) Regular MTSF models: including DLinear (Zeng et al. 2023), TimesNet (Wu et al. 2023), PatchTST (Nie et al. 2023), Crossformer (Wang et al. 2022), Graph Wavenet (Wu et al. 2019), MTGNN (Wu et al. 2020), StemGNN (Cao et al. 2020), CrossGNN (Huang et al. 2023), and FourierGNN (Yi et al. 2023). (2) IMTS classification/imputation models: including GRU-D (Che et al. 2018), SeFT (Horn et al. 2020), RainDrop (Zhang et al. 2022), Warperformer (Zhang et al. 2023), and mTAND (Shukla and Marlin 2021). (3) IMTSF models: including Latent ODEs (Rubanova, Chen, and Duvenaud 2019), CRU (Schirmer et al. 2022), and Neural Flows (Bilos et al. 2021), T-PATCHGNN (Zhang et al. 2024), and TimeCHEAT (Liu, Cao, and Chen 2025). For detailed information on the baseline models, please refer to Appendix A.2.

Implementation Details: We implement APN and all related experiments using the PyTorch framework on a server equipped with an Intel(R) Xeon(R) Gold 6326 CPU (@ 2.90GHz) and an NVIDIA GeForce RTX 3090 GPU. For our APN model, we set the hidden dimension D according to different datasets. Specifically, the hidden dimension D is set to 64 for the PhysioNet and USHCN, while it is set to 16 for the Human Activity and MIMIC. The time encoding dimension D_{te} is uniformly set to 10. The number of patches P is adjusted based on the characteristics of the datasets: 20 for PhysioNet, 16 for MIMIC, 75 for Human Activity, and 4 for USHCN. The training batch size is set to 256 for all datasets. The model is trained using the Adam optimizer with an initial learning rate of 1×10^{-2} . We train the model for a maximum of 200 epochs and employ an early stopping strategy with a patience of 50. To ensure the robustness of the results, we repeat each experiment 5 times using five different random seeds. We then report the mean and standard deviation of the performance metrics across these runs.

| Dataset | PhysioNet | | MIMIC | | Human Activity | | USHCN | |
|---------------|-----------------------------------|-----------------------------------|-----------------------------------|-----------------------------------|-----------------------------------|-----------------------------------|-----------------------------------|-----------------------------------|
| Metric | MSE $\times 10^{-3}$ | MAE $\times 10^{-2}$ | MSE $\times 10^{-2}$ | MAE $\times 10^{-2}$ | MSE $\times 10^{-3}$ | MAE $\times 10^{-2}$ | MSE $\times 10^{-1}$ | MAE $\times 10^{-1}$ |
| DLinear | 41.86 \pm 0.05 | 15.52 \pm 0.03 | 4.90 \pm 0.00 | 16.29 \pm 0.05 | 4.03 \pm 0.01 | 4.21 \pm 0.01 | 6.21 \pm 0.00 | 3.88 \pm 0.02 |
| TimesNet | 16.48 \pm 0.11 | 6.14 \pm 0.03 | 5.88 \pm 0.08 | 13.62 \pm 0.07 | 3.12 \pm 0.01 | 3.56 \pm 0.02 | 5.58 \pm 0.05 | 3.60 \pm 0.04 |
| PatchTST | 12.00 \pm 0.23 | 6.02 \pm 0.14 | 3.78 \pm 0.03 | 12.43 \pm 0.10 | 4.29 \pm 0.14 | 4.80 \pm 0.09 | 5.75 \pm 0.01 | 3.57 \pm 0.02 |
| Crossformer | 6.66 \pm 0.11 | 4.81 \pm 0.11 | 2.65 \pm 0.10 | 9.56 \pm 0.29 | 4.29 \pm 0.20 | 4.89 \pm 0.17 | 5.25 \pm 0.04 | 3.27 \pm 0.09 |
| Graph Wavenet | 6.04 \pm 0.28 | 4.41 \pm 0.11 | 2.93 \pm 0.09 | 10.50 \pm 0.15 | 2.89 \pm 0.03 | 3.40 \pm 0.05 | 5.29 \pm 0.04 | 3.16 \pm 0.09 |
| MTGNN | 6.26 \pm 0.18 | 4.46 \pm 0.07 | 2.71 \pm 0.23 | 9.55 \pm 0.65 | 3.03 \pm 0.03 | 3.53 \pm 0.03 | 5.39 \pm 0.05 | 3.34 \pm 0.02 |
| StemGNN | 6.86 \pm 0.28 | 4.76 \pm 0.19 | 1.73 \pm 0.02 | 7.71 \pm 0.11 | 8.81 \pm 0.37 | 6.90 \pm 0.02 | 5.75 \pm 0.09 | 3.40 \pm 0.09 |
| CrossGNN | 7.22 \pm 0.36 | 4.96 \pm 0.12 | 2.95 \pm 0.16 | 10.82 \pm 0.21 | 3.03 \pm 0.10 | 3.48 \pm 0.08 | 5.66 \pm 0.04 | 3.53 \pm 0.05 |
| FourierGNN | 6.84 \pm 0.35 | 4.65 \pm 0.12 | 2.55 \pm 0.03 | 10.22 \pm 0.08 | 2.99 \pm 0.02 | 3.42 \pm 0.02 | 5.82 \pm 0.06 | 3.62 \pm 0.07 |
| GRU-D | 5.59 \pm 0.09 | 4.08 \pm 0.05 | 1.76 \pm 0.03 | 7.53 \pm 0.09 | 2.94 \pm 0.05 | 3.53 \pm 0.06 | 5.54 \pm 0.38 | 3.40 \pm 0.28 |
| SeFT | 9.22 \pm 0.18 | 5.40 \pm 0.08 | 1.87 \pm 0.01 | 7.84 \pm 0.08 | 12.20 \pm 0.17 | 8.43 \pm 0.07 | 5.80 \pm 0.19 | 3.70 \pm 0.11 |
| RainDrop | 9.82 \pm 0.08 | 5.57 \pm 0.06 | 1.99 \pm 0.03 | 8.27 \pm 0.07 | 14.92 \pm 0.14 | 9.45 \pm 0.05 | 5.78 \pm 0.22 | 3.67 \pm 0.17 |
| Warpformer | 5.94 \pm 0.35 | 4.21 \pm 0.12 | 1.73 \pm 0.04 | 7.58 \pm 0.13 | 2.79 \pm 0.04 | 3.39 \pm 0.03 | 5.25 \pm 0.05 | 3.23 \pm 0.05 |
| APN (ours) | 4.48 \pm 0.06 | 3.43 \pm 0.02 | 1.61 \pm 0.02 | 6.82 \pm 0.05 | 2.71 \pm 0.00 | 3.10 \pm 0.01 | 4.52 \pm 0.06 | 2.92 \pm 0.05 |

Table 1: Overall performance evaluated by MSE and MAE (mean \pm std). The best-performing and second-best results are highlighted in **bold** and underline, respectively.

4.2 Main results

We compare the APN model with nineteen baseline models on four challenging datasets—see Table 1. We have the following observations: 1) APN achieves leading prediction accuracy across the board. On all datasets, APN achieves optimal or highly competitive forecasting performance. Compared to the second-best performing model, T-PATCHGNN, APN achieves significant reductions in MSE and MAE metrics by approximately 9.63% and 5.24%, respectively. 2) APN demonstrates exceptional cross-domain generalization capability and robustness. Whether on IMTS datasets with different characteristics in healthcare (PhysioNet, MIMIC), biomechanics (Human Activity), or climate science (USHCN), APN consistently performs excellently. The outstanding performance of APN can be attributed to its TAPA module, which generates superior patch representations by directly performing a soft-aggregation over raw observations within adaptively learned temporal windows. This approach effectively captures salient local dynamics without the potential distortion from interpolation. Building on these high-quality representations, the streamlined query module and MLP decoder ensure a lightweight yet powerful framework.

4.3 Ablation Studies

We perform ablation studies to isolate and validate the contribution of each primary component of APN. The complete results are provided in the Appendix B.2, with a representative summary presented in Table 2. The experiments yield three key observations. First, removing the *Adaptive Patching* mechanism and reverting to fixed-size windows results in a consistent decline in performance, which highlights the value of dynamically learned boundaries. Second, ablat-

| Dataset | PhysioNet | MIMIC | USHCN |
|-----------------------------------|-----------------------------------|-----------------------------------|-----------------------------------|
| Metric | MSE $\times 10^{-3}$ | MSE $\times 10^{-2}$ | MSE $\times 10^{-1}$ |
| w/o Adaptive Patching | 6.98 \pm 0.05 | 2.05 \pm 0.02 | 5.59 \pm 0.05 |
| w/o Weighted Aggregation | 9.92 \pm 0.11 | 2.27 \pm 0.03 | 5.38 \pm 0.02 |
| w/o Query-based Patch Aggregation | 9.92 \pm 0.10 | 3.57 \pm 0.03 | 5.21 \pm 0.04 |
| APN (ours) | 4.48 \pm 0.06 | 1.61 \pm 0.02 | 4.52 \pm 0.06 |

Table 2: Ablation studies for APN in terms of the best result highlighted in **bold**.

ing the *Weighted Aggregation* scheme for a simple average over hard-cut patches leads to the most significant performance degradation. This empirically confirms that our soft-aggregation design is critical for preventing information loss at patch boundaries (i.e., the coverage issue). Third, replacing the *Query-Based Patch Aggregation* with a basic linear layer also diminishes performance, proving that our sophisticated aggregation method is essential for integrating contextual information within variables.

4.4 Parameter Sensitivity

To gain a deeper understanding of the impact of key hyperparameters on the performance of the APN model, we conduct parameter sensitivity analyses, focusing primarily on the number of patches (P), the model’s hidden dimension (D), and the time encoding dimension (D_{te})—see Figure 3. We have the following observations: 1) From Figures 3a and 3b, we observe that for most datasets, a larger P does not

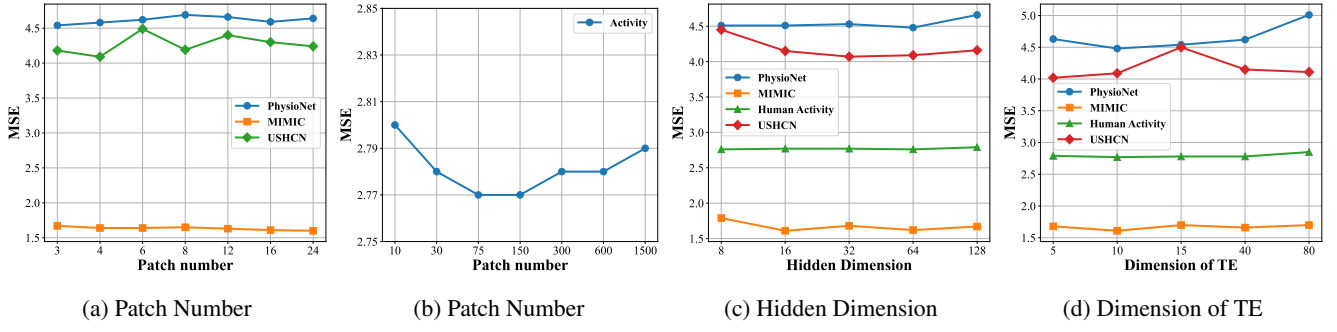


Figure 3: Parameter sensitivity studies of main hyper-parameters in APN

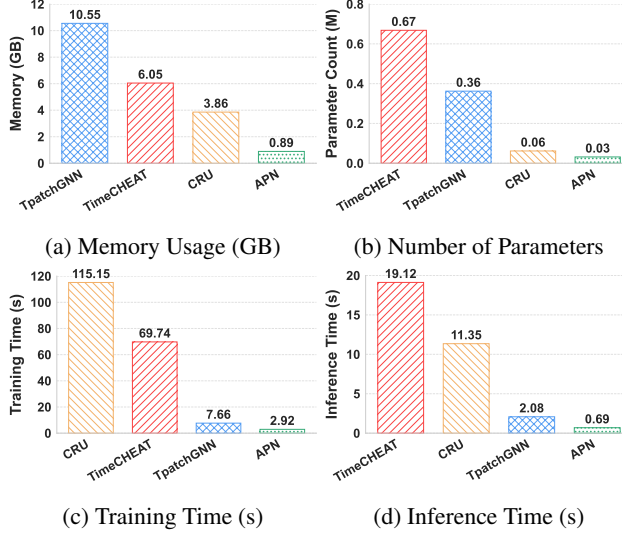


Figure 4: We evaluate the memory usage (GB), number of parameters (M), average training time per epoch (s), and total inference time (s) of APN and three representative baselines for IMTSF. All experiments are conducted on the PhysioNet dataset with a consistent batch size of 32 to ensure fair comparison. A lower value indicates better performance.

necessarily lead to better performance. This suggests that an appropriate P value can better balance the capture of local information and model complexity. 2) Figure 3c reveals the impact of the model’s hidden dimension (D). In general, a smaller hidden dimension may already be sufficient to capture effective information, while an excessively large dimension can sometimes lead to a slight performance decline. This indicates that the choice of D should be comprehensively considered based on the scale and sparsity of the dataset. 3) Figure 3d shows the influence of the time encoding dimension (D_{te}). The results indicate that a moderate D_{te} value can provide the model with effective temporal information. An excessively high time encoding dimension may introduce too much noise, interfering with the learning of core features. 4) The APN model exhibits a certain sensitivity to the selection of these core hyperparameters, but it generally achieves competitive results within a reasonable range. In practical applications, appropriate tuning should be performed based on the specific characteristics of the dataset.

In practical applications, appropriate tuning should be performed based on the specific characteristics of the dataset.

4.5 Scalability and Efficiency Analysis

To comprehensively evaluate the potential of APN in practical deployment, we conduct a comparative analysis of computational efficiency and resource consumption between APN and three representative baseline models (TimeCHEAT (Liu, Cao, and Chen 2025), CRU (Schirmer et al. 2022), T-PatchGNN (Zhang et al. 2024)) on the PhysioNet dataset, with the batch size uniformly set to 32—see Figure 4. The results demonstrate that APN exhibits significant advantages across all key efficiency metrics. This is attributed to its core TAPA module, which efficiently generates information-condensed and regularized initial representations. These representations support a highly streamlined information aggregation and prediction architecture, ultimately achieving a lightweight and highly efficient model design.

5 Conclusion

This paper addresses the challenges of IMTS forecasting by proposing a general and efficient framework, APN. The core of APN lies in its novel Time-Aware Patch Aggregation (TAPA) module. This module introduces an aggregation-based paradigm, distinct from methods that rely on fixed patching or interpolation. By learning dynamic boundaries and applying a time-aware soft-weighting strategy, TAPA directly aggregates information from all raw observations to generate high-quality, regularized patch representations. This design choice not only ensures full data coverage and robustly handles information density variations, but also enables a streamlined and efficient overall architecture. Leveraging these superior representations, APN employs a concise query module and a shallow MLP to make predictions. Extensive experiments on multiple public IMTS benchmark datasets demonstrate that APN significantly outperforms existing state-of-the-art methods in both prediction accuracy and computational efficiency.

References

- Bilos, M.; Sommer, J.; Rangapuram, S. S.; Januschowski, T.; and Günemann, S. 2021. Neural Flows: Efficient Alternative to Neural ODEs. In *Advances in Neural Information Processing Systems 34: Annual Conference on Neural Information Processing Systems 2021, NeurIPS 2021, December 6-14, 2021, virtual*, 21325–21337.
- Brouwer, E. D.; Simm, J.; Arany, A.; and Moreau, Y. 2019. GRU-ODE-Bayes: Continuous Modeling of Sporadically-Observed Time Series. In *Advances in Neural Information Processing Systems 32: Annual Conference on Neural Information Processing Systems 2019, NeurIPS 2019, December 8-14, 2019, Vancouver, BC, Canada*, 7377–7388.
- Cao, D.; Wang, Y.; Duan, J.; Zhang, C.; Zhu, X.; Huang, C.; Tong, Y.; Xu, B.; Bai, J.; Tong, J.; and Zhang, Q. 2020. Spectral Temporal Graph Neural Network for Multivariate Time-series Forecasting. In *Advances in Neural Information Processing Systems 33: Annual Conference on Neural Information Processing Systems 2020, NeurIPS 2020, December 6-12, 2020, virtual*.
- Che, Z.; Purushotham, S.; Cho, K.; Sontag, D.; and Liu, Y. 2018. Recurrent neural networks for multivariate time series with missing values. *Scientific reports*, 8(1): 6085.
- Chen, T. Q.; Rubanova, Y.; Bettencourt, J.; and Duvenaud, D. 2018. Neural Ordinary Differential Equations. In *Advances in Neural Information Processing Systems 31: Annual Conference on Neural Information Processing Systems 2018, NeurIPS 2018, December 3-8, 2018, Montréal, Canada*, 6572–6583.
- Chen, Y.; Ren, K.; Wang, Y.; Fang, Y.; Sun, W.; and Li, D. 2023. ContiFormer: Continuous-Time Transformer for Irregular Time Series Modeling. In *Advances in Neural Information Processing Systems 36: Annual Conference on Neural Information Processing Systems 2023, NeurIPS 2023, New Orleans, LA, USA, December 10 - 16, 2023*.
- Gravina, A.; Zambon, D.; Bacciu, D.; and Alippi, C. 2024. Temporal Graph ODEs for Irregularly-Sampled Time Series. In *Proceedings of the Thirty-Third International Joint Conference on Artificial Intelligence, IJCAI 2024, Jeju, South Korea, August 3-9, 2024*, 4025–4034.
- Ham, Y.; Kim, J.; and Luo, J. 2019. Deep learning for multi-year ENSO forecasts. *Nat.*, 573(7775): 568–572.
- Horn, M.; Moor, M.; Bock, C.; Rieck, B.; and Borgwardt, K. M. 2020. Set Functions for Time Series. In *Proceedings of the 37th International Conference on Machine Learning, ICML 2020, 13-18 July 2020, Virtual Event*, volume 119 of *Proceedings of Machine Learning Research*, 4353–4363.
- Huang, Q.; Shen, L.; Zhang, R.; Cheng, J.; Ding, S.; Zhou, Z.; and Wang, Y. 2024. HDMixer: Hierarchical Dependency with Extendable Patch for Multivariate Time Series Forecasting. In *Proceedings of the AAAI Conference on Artificial Intelligence 38: AAAI Conference on Artificial Intelligence 2024, AAAI 2024*, 12608–12616.
- Huang, Q.; Shen, L.; Zhang, R.; Ding, S.; Wang, B.; Zhou, Z.; and Wang, Y. 2023. CrossGNN: Confronting Noisy Multivariate Time Series Via Cross Interaction Refinement. In *Advances in Neural Information Processing Systems 36: Annual Conference on Neural Information Processing Systems 2023, NeurIPS 2023, New Orleans, LA, USA, December 10 - 16, 2023*.
- Kidger, P.; Morrill, J.; Foster, J.; and Lyons, T. J. 2020. Neural Controlled Differential Equations for Irregular Time Series. In *Advances in Neural Information Processing Systems 33: Annual Conference on Neural Information Processing Systems 2020, NeurIPS 2020, December 6-12, 2020, virtual*.
- Kim, D.; Park, J.; Lee, J.; and Kim, H. 2024. Are Self-Attentions Effective for Time Series Forecasting? In *Advances in Neural Information Processing Systems 38: Annual Conference on Neural Information Processing Systems 2024, NeurIPS 2024, Vancouver, BC, Canada, December 10 - 15, 2024*.
- Lin, S.; Lin, W.; Hu, X.; Wu, W.; Mo, R.; and Zhong, H. 2024a. CycleNet: Enhancing Time Series Forecasting through Modeling Periodic Patterns. In *Advances in Neural Information Processing Systems 38: Annual Conference on Neural Information Processing Systems 2024, NeurIPS 2024, Vancouver, BC, Canada, December 10 - 15, 2024*.
- Lin, S.; Lin, W.; Wu, W.; Chen, H.; and Yang, J. 2024b. SparseTSF: Modeling Long-term Time Series Forecasting with *1k* Parameters. In *Forty-first International Conference on Machine Learning, ICML 2024, Vienna, Austria, July 21-27, 2024*.
- Liu, J.; Cao, M.; and Chen, S. 2025. TimeCHEAT: A Channel Harmony Strategy for Irregularly Sampled Multivariate Time Series Analysis. In *AAAI-25, Sponsored by the Association for the Advancement of Artificial Intelligence, February 25 - March 4, 2025, Philadelphia, PA, USA*, 18861–18869.
- Nie, Y.; Nguyen, N. H.; Sinhong, P.; and Kalagnanam, J. 2023. A Time Series is Worth 64 Words: Long-term Forecasting with Transformers. In *The Eleventh International Conference on Learning Representations, ICLR 2023, Kigali, Rwanda, May 1-5, 2023*.
- Rubanova, Y.; Chen, T. Q.; and Duvenaud, D. 2019. Latent Ordinary Differential Equations for Irregularly-Sampled Time Series. In *Advances in Neural Information Processing Systems 32: Annual Conference on Neural Information Processing Systems 2019, NeurIPS 2019, December 8-14, 2019, Vancouver, BC, Canada*, 5321–5331.
- Schirmer, M.; Eltayeb, M.; Lessmann, S.; and Rudolph, M. 2022. Modeling Irregular Time Series with Continuous Recurrent Units. In *International Conference on Machine Learning, ICML 2022, 17-23 July 2022, Baltimore, Maryland, USA*, volume 162 of *Proceedings of Machine Learning Research*, 19388–19405.
- Shukla, S. N.; and Marlin, B. M. 2021. Multi-Time Attention Networks for Irregularly Sampled Time Series. In *9th International Conference on Learning Representations, ICLR 2021, Virtual Event, Austria, May 3-7, 2021*.
- Vio, R.; Díaz-Trigo, M.; and Andreani, P. 2013. Irregular time series in astronomy and the use of the Lomb-Scargle periodogram. *Astron. Comput.*, 1: 5–16.

- Wang, W.; Yao, L.; Chen, L.; Lin, B.; Cai, D.; He, X.; and Liu, W. 2022. CrossFormer: A Versatile Vision Transformer Hinging on Cross-scale Attention. In *The Tenth International Conference on Learning Representations, ICLR 2022, Virtual Event, April 25-29, 2022*.
- Wu, H.; Hu, T.; Liu, Y.; Zhou, H.; Wang, J.; and Long, M. 2023. TimesNet: Temporal 2D-Variation Modeling for General Time Series Analysis. In *The Eleventh International Conference on Learning Representations, ICLR 2023, Kigali, Rwanda, May 1-5, 2023*.
- Wu, Z.; Pan, S.; Chen, F.; Long, G.; Zhang, C.; and Yu, P. S. 2021. A Comprehensive Survey on Graph Neural Networks. *IEEE Trans. Neural Networks Learn. Syst.*, 32(1): 4–24.
- Wu, Z.; Pan, S.; Long, G.; Jiang, J.; Chang, X.; and Zhang, C. 2020. Connecting the Dots: Multivariate Time Series Forecasting with Graph Neural Networks. In *KDD '20: The 26th ACM SIGKDD Conference on Knowledge Discovery and Data Mining, Virtual Event, CA, USA, August 23-27, 2020*, 753–763.
- Wu, Z.; Pan, S.; Long, G.; Jiang, J.; and Zhang, C. 2019. Graph WaveNet for Deep Spatial-Temporal Graph Modeling. In *Proceedings of the Twenty-Eighth International Joint Conference on Artificial Intelligence, IJCAI 2019, Macao, China, August 10-16, 2019*, 1907–1913.
- Yalavarthi, V. K.; Madhusudhanan, K.; Scholz, R.; Ahmed, N.; Burchert, J.; Jawed, S.; Born, S.; and Schmidt-Thieme, L. 2024. GraFITi: Graphs for Forecasting Irregularly Sampled Time Series. In *Thirty-Eighth AAAI Conference on Artificial Intelligence, AAAI 2024, Thirty-Sixth Conference on Innovative Applications of Artificial Intelligence, IAAI 2024, Fourteenth Symposium on Educational Advances in Artificial Intelligence, EAAI 2024, February 20-27, 2024, Vancouver, Canada*, 16255–16263.
- Yao, Z.; Bi, J.; and Chen, Y. 2018. Applying Deep Learning to Individual and Community Health Monitoring Data: A Survey. *Int. J. Autom. Comput.*, 15(6): 643–655.
- Yi, K.; Zhang, Q.; Fan, W.; He, H.; Hu, L.; Wang, P.; An, N.; Cao, L.; and Niu, Z. 2023. FourierGNN: Rethinking Multivariate Time Series Forecasting from a Pure Graph Perspective. In *Advances in Neural Information Processing Systems 36: Annual Conference on Neural Information Processing Systems 2023, NeurIPS 2023, New Orleans, LA, USA, December 10 - 16, 2023*.
- Zeng, A.; Chen, M.; Zhang, L.; and Xu, Q. 2023. Are Transformers Effective for Time Series Forecasting? In *Thirty-Seventh AAAI Conference on Artificial Intelligence, AAAI 2023, Thirty-Fifth Conference on Innovative Applications of Artificial Intelligence, IAAI 2023, Thirteenth Symposium on Educational Advances in Artificial Intelligence, EAAI 2023, Washington, DC, USA, February 7-14, 2023*, 11121–11128.
- Zhang, J.; Zheng, S.; Cao, W.; Bian, J.; and Li, J. 2023. Warpformer: A Multi-scale Modeling Approach for Irregular Clinical Time Series. In *Proceedings of the 29th ACM SIGKDD Conference on Knowledge Discovery and Data Mining, KDD 2023, Long Beach, CA, USA, August 6-10, 2023*, 3273–3285.
- Zhang, W.; Yin, C.; Liu, H.; Zhou, X.; and Xiong, H. 2024. Irregular Multivariate Time Series Forecasting: A Transformable Patching Graph Neural Networks Approach. In *Forty-first International Conference on Machine Learning, ICML 2024, Vienna, Austria, July 21-27, 2024*.
- Zhang, X.; Zeman, M.; Tsilgkaridis, T.; and Zitnik, M. 2022. Graph-Guided Network for Irregularly Sampled Multivariate Time Series. In *The Tenth International Conference on Learning Representations, ICLR 2022, Virtual Event, April 25-29, 2022*.